Article

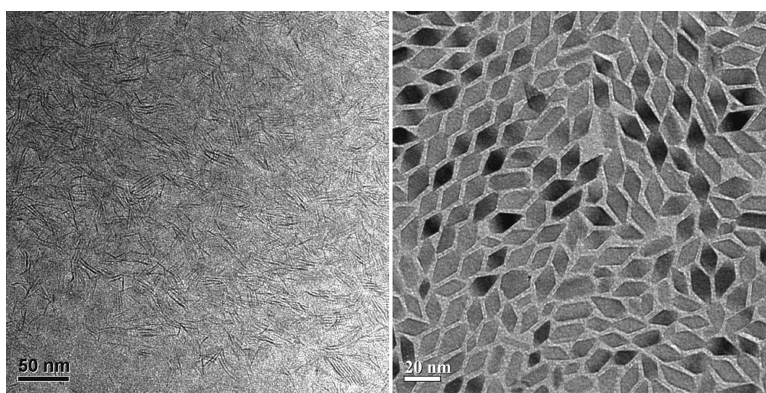# Nonaqueous Production of Nanostructured Anatase with High-Energy Facets

Binghui Wu, Changyou Guo, Nanfeng Zheng, Zhaoxiong Xie, and Galen D. Stucky

More About This Article

Additional resources and features associated with this article are available within the HTML version:

- Supporting Information
- Access to high resolution figures
- Links to articles and content related to this article
- Copyright permission to reproduce figures and/or text from this article

View the Full Text HTML

Nonaqueous Production of Nanostructured Anatase with High-Energy Facets

Binghui Wu,[†] Changyou Guo,[†] Nanfeng Zheng,*,[†] Zhaoxiong Xie,[†] and Galen D. Stucky*,[‡]

State Key Laboratory for Physical Chemistry of Solid Surfaces and Department of Chemistry, Xiamen University, Xiamen 361005, China, and Department of Chemistry and Biochemistry, University of California, Santa Barbara, California 93106

Received September 3, 2008; E-mail: nfzheng@xmu.edu.cn; stucky@chem.ucsb.edu

Abstract: Although solution-based synthesis is the most powerful and economic method to create nanostructured anatase TiO$_2$, under those synthesis conditions the {101} facets are the most thermodynamically stable, making it difficult to create anatase nanomaterials with a large percentage of high-energy {001} or {010} facets exposed. Here, we report a facile nonaqueous synthetic route to prepare anatase nanosheets with exposed {001} facets and high-quality rhombic-shaped anatase nanocrystals with a large percentage of exposed {010} facets. Including adscititious water in the nonaqueous synthesis and eliminating the use of carboxylic acid type capping agents are the two keys to integrating the structural diversity from aqueous systems into large-quantity synthesis in nonaqueous systems. The nanostructured TiO$_2$ that we prepared exhibits conspicuous activity in the photocatalytic degradation of organic contaminants.

Introduction

The chemistry of titania has received much scientific and technological attention owing to its widespread applications in fields such as solar energy conversion, photocatalysis, optics, catalysis, photochromic devices, and gas sensing.[1−5] Nanostructured TiO$_2$ has been playing an increasing role in these applications where crystal structure, size, and shape are important.[4] For example, the photocatalytic/photovoltaic properties of TiO$_2$ nanoparticles are strongly dependent on the surface area, the exposed surface, and the crystallinity of the particles.[2,6]

Recently, there have been many reports on the synthesis of TiO$_2$ nanomaterials using sol−gel,[7−13] nonaqueous sol,[14−23] micelle /reverse micelle,[24−28] polyol,[29] sonochemical synthesis,[30,31] a hydro-/solvothermal method,[32−35] and other techniques.[4] Among these methods, titanium alkoxides are widely used as the titania precursors. Due to the high reactivity of these precursors, delicate control over reaction conditions is essential

† Xiamen University.
‡ University of California.

 (1) Fujishima, A.; Honda, K. *Nature* **1972**, *238*, 37–38.
 (2) Grätzel, M. *Nature* **2001**, *414*, 338–344.
 (3) Barbe, C. J.; Arendse, F.; Comte, P.; Jirousek, M.; Lenzmann, F.; Shklover, V.; Grätzel, M. *J. Am. Ceram. Soc.* **1997**, *80*, 3157–3171.
 (4) Chen, X.; Mao, S. S. *Chem. Rev.* **2007**, *107*, 2891–2959.
 (5) O'Regan, B.; Grätzel, M. *Nature* **1991**, *353*, 737–740.
 (6) Hagfeldt, A.; Grätzel, M. *Chem. Rev.* **1995**, *95*, 49–68.
 (7) Moritz, T.; Reiss, J.; Diesner, K.; Su, D.; Chemseddine, A. *J. Phys. Chem. B* **1997**, *101*, 8052–8053.
 (8) Chemseddine, A.; Moritz, T. *Eur. J. Inorg. Chem.* **1999**, 235–245.
 (9) Oskam, G.; Nellore, A.; Penn, R. L.; Searson, P. C. *J. Phys. Chem. B* **2003**, *107*, 1734–1738.
(10) Chen, Q.; Zhou, W. Z.; Du, G. H.; Peng, L. M. *Adv. Mater.* **2002**, *14*, 1208–1211.
(11) Pottier, A. S.; Cassaignon, S.; Chaneac, C.; Villain, F.; Tronc, E.; Jolivet, J. P. *J. Mater. Chem.* **2003**, *13*, 877–882.
(12) Antonelli, D. M.; Ying, J. Y. *Angew. Chem., Int. Ed.* **1995**, *34*, 2014–2017.
(13) Bartl, M. H.; Boettcher, S. W.; Frindell, K. L.; Stucky, G. D. *Acc. Chem. Res.* **2005**, *38*, 263–271.
(14) Jun, Y. W.; Casula, M. F.; Sim, J. H.; Kim, S. Y.; Cheon, J.; Alivisatos, A. P. *J. Am. Chem. Soc.* **2003**, *125*, 15981–15985.
(15) Cozzoli, P. D.; Kornowski, A.; Weller, H. *J. Am. Chem. Soc.* **2003**, *125*, 14539–14548.
(16) Joo, J.; Kwon, S. G.; Yu, T.; Cho, M.; Lee, J.; Yoon, J.; Hyeon, T. *J. Phys. Chem. B* **2005**, *109*, 15297–15302.
(17) Zhang, Z. H.; Zhong, X. H.; Liu, S. H.; Li, D. F.; Han, M. Y. *Angew. Chem., Int. Ed.* **2005**, *44*, 3466–3470.
(18) Vioux, A. *Chem. Mater.* **1997**, *9*, 2292–2299.
(19) Seo, J. W.; Jun, Y. W.; Ko, S. J.; Cheon, J. *J. Phys. Chem. B* **2005**, *109*, 5389–5391.
(20) Trentler, T. J.; Denler, T. E.; Bertone, J. F.; Agrawal, A.; Colvin, V. L. *J. Am. Chem. Soc.* **1999**, *121*, 1613–1614.
(21) Niederberger, M. *Acc. Chem. Res.* **2007**, *40*, 793–800.
(22) Niederberger, M.; Bartl, M. H.; Stucky, G. D. *Chem. Mater.* **2002**, *14*, 4364–4370.
(23) Niederberger, M.; Bartl, M. H.; Stucky, G. D. *J. Am. Chem. Soc.* **2002**, *124*, 13642–13643.
(24) Li, Y. Z.; Lee, N. H.; Hwang, D. S.; Song, J. S.; Lee, E. G.; Kim, S. J. *Langmuir* **2004**, *20*, 10838–10844.
(25) Lin, J.; Lin, Y.; Liu, P.; Meziani, M. J.; Allard, L. F.; Sun, Y. P. *J. Am. Chem. Soc.* **2002**, *124*, 11514–11518.
(26) Wu, M. M.; Long, J. B.; Huang, A. H.; Luo, Y. J.; Feng, S. H.; Xu, R. R. *Langmuir* **1999**, *15*, 8822–8825.
(27) Stathatos, E.; Lianos, P.; Del Monte, F.; Levy, D.; Tsiourvas, D. *Langmuir* **1997**, *13*, 4295–4300.
(28) Zhang, D. B.; Qi, L. M.; Ma, J. M.; Cheng, H. M. *J. Mater. Chem.* **2002**, *12*, 3677–3680.
(29) Feldmann, C.; Jungk, H. O. *Angew. Chem., Int. Ed.* **2001**, *40*, 359–362.
(30) Zhu, Y. C.; Li, H. L.; Koltypin, Y.; Hacohen, Y. R.; Gedanken, A. *Chem. Commun.* **2001**, 2616–2617.
(31) Yu, J. C.; Yu, J. G.; Ho, W. K.; Zhang, L. Z. *Chem. Commun.* **2001**, 1942–1943.
(32) Bacsa, R. R.; Grätzel, M. *J. Am. Ceram. Soc.* **1996**, *79*, 2185–2188.
(33) Penn, R. L.; Banfield, J. F. *Geochim. Cosmochim. Acta* **1999**, *63*, 1549–1557.
(34) Li, X. L.; Peng, Q.; Yi, J. X.; Wang, X.; Li, Y. D. *Chem.—Eur. J.* **2006**, *12*, 2383–2391.
(35) Zaban, A.; Aruna, S. T.; Tirosh, S.; Gregg, B. A.; Mastai, Y. *J. Phys. Chem. B* **2000**, *104*, 4130–4133.

to obtain nanocrystals with specific size and shape in solution-based synthesis. In aqueous systems, the use of alkoxide precursors in a low concentration has become a widely recognized condition to prevent nanocrystals from aggregation and/or further growth, which makes it difficult to achieve the large-quantity preparation of high-quality and uniform TiO$_2$ nanocrystals.[7−11]

Therefore, much research effort has been directed to the development of nonaqueous synthetic routes in which TiO$_2$ precursors can be supplied in much higher concentrations.[14−22,34] By choosing appropriate solvents, the nonaqueous synthesis of nanostructured TiO$_2$ can be accomplished with or without the help of surfactants or capping agents. For example, Niederberger and co-workers have extensively demonstrated that benzyl alcohol is an excellent reaction medium to prepare a wide range of metal-oxide nanostructures without the use of any additional surfactant or capping agent.[22,23,36−39] Nevertheless, under such conditions, the morphology of obtained metal-oxide nanostructures is rather limited. To gain TiO$_2$ nanostructures with better-controlled size and shape, the use of capping ligands is essentially critical. In nonaqueous synthesis, however, capping agents have been overwhelmingly dominated by carboxylic acids.[14−19,34] Due to their tight binding on the TiO$_2$ surface, the use of carboxylic acids restrains the crystal growth, particularly for the high-energy facets exposed. As a result, TiO$_2$ nanocrystals prepared nonaqueously are limited to spherical, diamond-shaped, and rod-like particles with low-energy facets exposed. In comparison, anatase nanocrystals prepared from aqueous systems are much more diverse in morphology.[8,40] Therefore, an important issue to be addressed in nonaqueous synthesis of nanoscale TiO$_2$ is how to create nanostructures that are currently achievable only by aqueous routes.

We have now developed a synthetic strategy that allows the integration of structural diversity from aqueous systems into large-quantity synthesis in nonaqueous systems. Together with the exclusion of carboxylic acid type capping agents, the inclusion of adscititious water in the nonaqueous synthesis is demonstrated as the key for the large-quantity production of nanostructured anatase with exposed high-energy facets (i.e., {001}, {010}) and therefore excellent photocatalytic properties. It should be noted that nanomaterials with high-energy facets have emerged as attractive candidates for many catalysis and photocatalysis applications.[41−43] However, they are generally

difficult to produce by conventional physical and chemical methods because of their high reactivities during preparation.[44,45]

Experimental Section

Synthesis of *NS*-TiO$_2$. 5 mL of benzyl alcohol (BA), 2 mL of oleylamine (OA), and 0.25 mL of titanium isopropoxide (TIPO) were mixed in a dried Teflon autoclave and stirred for 10 min at room temperature. The vessel was then sealed and heated at 180 °C for 24 h. After cooled to room temperature, the resultant pale yellow milky suspensions were precipitated by absolute ethanol and separated via centrifugation. The pale yellow products were purified by three successive cycles of dispersion in chloroform, precipitation with ethanol, and centrifugation (6000 rpm, 3 min).

Synthesis of *NC*-TiO$_2$. Rhombic anatase TiO$_2$ nanocrystals were synthesized under conditions similar to that of *NS*-TiO$_2$ except that an appropriate amount of adscititious water (e.g., 60 μL, 100 μL) was added to the reactions. The off-white precipitation was purified by using a procedure similar to that for *NS*-TiO$_2$.

Preparation of the Water-Soluble Suspensions. 0.1−0.2 g of *NS*-TiO$_2$ or *NC*-TiO$_2$ were added to 20 mL of ethanol solution of tetrabutylammonium hydroxide (TBAOH) (0.4−0.8 g) and stirred for at least 3 days at room temperature to produce a stable colloidal suspension. The resulting dispersion was translucent to opalescent, depending on the content of titania. Then, the white products were separated via centrifugation (10 000 rpm, 5 min), purified by three successive cycles of ultrasonic treatment and centrifugation with ethanol, and last dispersed in water for measurements of photocatalytic activity and adsorption ability of methyl orange (MO).

Adsorption of MO on TiO$_2$ Nanocrystals. A 5 mg amount of treated TiO$_2$ was dispersed in 3 mL of water, mixed with 3 mL of 0.3 g/L MO, and shaken in the dark for 24 h. For comparison, the Degussa P25 sample was also used in the dye adsorption experiment. The MO-loaded TiO$_2$ was precipitated with centrifugation (15 000 rpm, 10 min); the upper layer was appropriately diluted and monitored by a UV spectrophotometer (UV-2501PC, Shimadzu) at 465 nm. The MO loading contents were calculated by the following equation:

$$\text{MO loading contents (\%)} = \frac{\text{weight of MO adsorbed on prepared nanoparticles}}{\text{weight of prepared nanoparticles}} \times 100 \quad (1)$$

Photocatalysis. Experiments of photocatalysis in the degradation of MO (50 μL, 1 mmol/L) were carried out in a quartz cell (using a small magneton for stirring) in the presence of TiO$_2$ photocatalysts (3 mL, 0.033 g/L) by UV light irradiation from a 300 W high-pressure mercury lamp. The degree of degradation was obtained at 465 nm by real time detection on a Halogen Light Source HL-2000 (Ocean Optics, Inc.).

Results and Discussion

Figure 1 shows two distinct types of nanostructured titania that have been prepared under solvothermal conditions by using TIPO as the titania precursor, a primary amine (e.g., oleylamine, 1-octylamine, 1-dodecylamine) as the capping agent, and BA as the reaction medium. In this nonaqueous system, adscititious water plays a significant role in controlling the growth of the titania structures. Nanostructured titania composed of nanosheets situated parallel to one another (denoted as *NS*-TiO$_2$) were obtained if no water was introduced into the reaction (Figure 1a−c). However, when an appropriate amount of adscititious water was supplied, the reaction led to the formation of uniform rhombic-shaped anatase nanocrystals (denoted as *NC*-TiO$_2$) (Figure 1d) of high-quality as revealed by HRTEM (Figure 1e).

For *NS*-TiO$_2$ prepared without the use of water, detailed TEM studies show that the slabs present in the structure are uniform in width (7.5 ± 1 Å), which is similar to titania slabs previously reported in aqueous solutions.[8] The interslab distance depends

(36) Pinna, N.; Niederberger, M. *Angew. Chem., Int. Ed.* **2008**, *47*, 5292–5304.
(37) Niederberger, M.; Garnweitner, G. *Chem.−Eur. J.* **2006**, *12*, 7282–7302.
(38) Niederberger, M.; Garnweitner, G.; Buha, J.; Polleux, J.; Ba, J.; Pinna, N. *J. Sol-Gel Sci. Technol.* **2006**, *40*, 259–266.
(39) Bilecka, I.; Djerdj, I.; Niederberger, M. *Chem. Commun.* **2008**, 886–888.
(40) Wen, P. H.; Itoh, H.; Tang, W. P.; Feng, Q. *Langmuir* **2007**, *23*, 11782–11790.
(41) Tian, N.; Zhou, Z. Y.; Sun, S. G.; Ding, Y.; Wang, Z. L. *Science* **2007**, *316*, 732–735.
(42) Diebold, U. *Surf. Sci. Rep.* **2003**, *48*, 53–229.
(43) Vittadini, A.; Casarin, M.; Selloni, A. *Theor. Chem. Acc.* **2007**, *117*, 663–671.
(44) Yang, H. G.; Sun, C. H.; Qiao, S. Z.; Zou, J.; Liu, G.; Smith, S. C.; Cheng, H. M.; Lu, G. Q. *Nature* **2008**, *453*, 638–641.
(45) Ding, K. L.; Miao, Z. J.; Liu, Z. M.; Zhang, Z. F.; Han, B. X.; An, G. M.; Miao, S. D.; Xie, Y. *J. Am. Chem. Soc.* **2007**, *129*, 6362–6363.
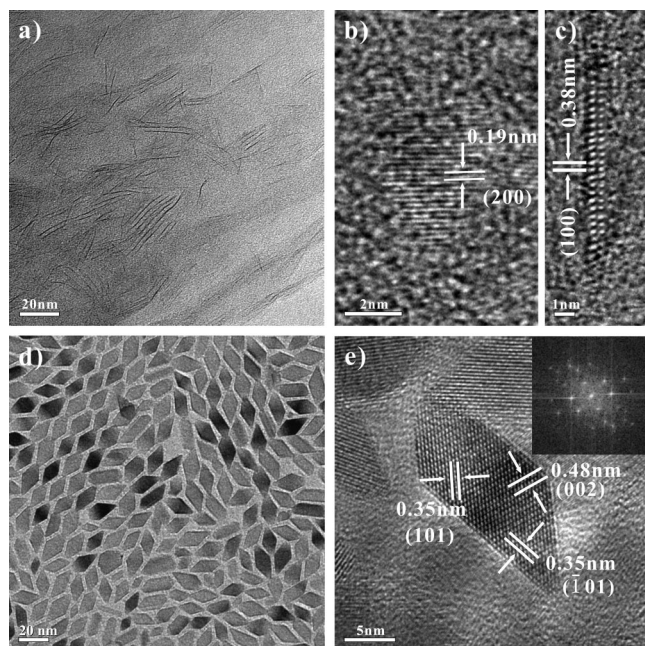
Figure 1. Representative TEM images of *NS*-TiO$_2$ and *NC*-TiO$_2$. (a) Low-magnification image of as-made *NS*-TiO$_2$. (b and c) High-magnification images of nanosheets obtained by treating *NS*-TiO$_2$ with TBAOH. (d and e) Low-magnification and high-resolution TEM images of *NC*-TiO$_2$. The inset in (e) is the Fourier transfer image corresponding to HRTEM of *NC*-TiO$_2$.

Figure 2. XRD patterns of products collected from the 24-h reactions at 180 °C with different water supply. Reactions conditions: BA 5 mL, OA 2 mL, TIPO 0.25 mL, different amounts of water (as labeled).

on the length of amines used in the synthesis (Figure S1). In the case of OA, a distance of 3.2 nm is revealed. Both TGA (Figure S2) and CNH elemental analysis results reveal the high content (ca. 43% in weight) of OA present in the as-prepared *NS*-TiO$_2$. The sheet thickness of ~7.5 Å as revealed by TEM indicates that each sheet is likely a single molecular sheet, similar to the slabs observed in aqueous synthesis.[8] However, the high content of OA in the as-made *NS*-TiO$_2$ holds the TiO$_2$ molecular sheet tightly into the lamellar structure and renders our efforts fruitless in obtaining good HRTEM images of *NS*-TiO$_2$. We then treated *NS*-TiO$_2$ powders with an ethanol solution of TBAOH to exfoliate *NS*-TiO$_2$. Such a treatment substitutes OA in *NS*-TiO$_2$ with TBA$^+$, resulting in the formation of a translucent colloidal suspension. The successful delamination of *NS*-TiO$_2$ allows us to obtain unambiguous HRTEM images on the molecular sheets (Figure 1b and 1c) which lie on or perpendicular to the TEM grid. Lattice fringes with the spacing of 0.19 nm (Figure 1b), corresponding to the (200) of anatase, can be clearly revealed from those sheets lying on the TEM grid. When lying perpendicular to the grid, a periodicity of 0.38 nm is revealed (Figure 1c), which is the spacing along the *a* or *b* axis of anatase.

In addition to TEM analysis, we have applied XRD to evaluate the bulk *NS*-TiO$_2$ samples. A typical small-angle XRD (SAXRD) pattern of lamellar TiO$_2$ is shown in Figure 2. A series of peaks at low angular range with a *d*-spacing of 31.9, 16.0 and 10.6, 8.0, 6.4 Å are observed, which indicates the lamellar ordering of TiO$_2$ nanosheets with an interlayer distance of 3.2 nm. In the wide-angle XRD (WAXRD) pattern of *NS*-TiO$_2$, two sets of diffraction peaks are observed. One set has relatively narrow and intense peaks located at 2θ of 48.3°, 62.7°, and 82.8°. The other set of peaks, located at 2θ of 25.4°, 38.7°, and 69.0°, are rather broad and weak. While the intense peaks can be attributed to anatase (200), (204), and (224) reflections, respectively, the weak peaks match well with (101), (004), and
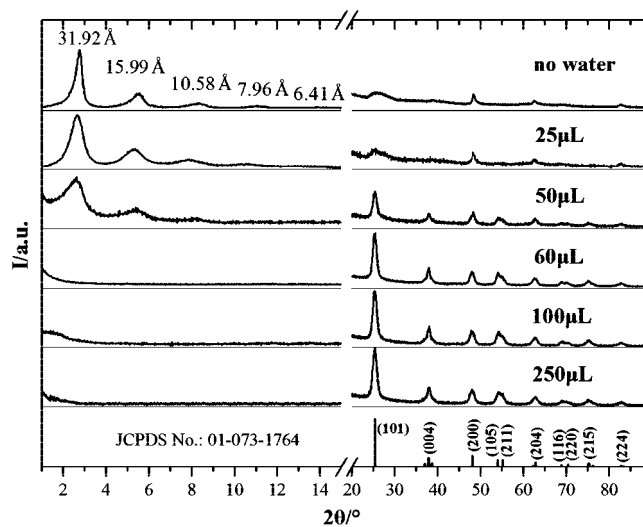
(116) of anatase, which is also revealed by the selected area electron diffraction (Figure S3). Such a diffraction pattern indicates the anatase feature within the titania nanosheets with preferential growth along the *a* or *b* axis and assembly along the [001] direction,[46] which is consistent with the HRTEM measurements discussed above.

Reaction temperature plays an important role in the formation of *NS*-TiO$_2$. Shown in Figure 3a are the XRD patterns of the products collected from the 24-h reactions run at 100, 150, 180, and 200 °C, respectively. The lack of featured diffraction peaks at both low and wide angles illustrates that neither *NS*-TiO$_2$ nor TiO$_2$ nanocrystals are observed in the reaction at 100 °C. The formation of *NS*-TiO$_2$ starts at 150 °C and becomes significant at 180 °C. Pure *NS*-TiO$_2$ can be obtained quantitatively from a 1-day reaction at 180 °C. However, when the temperature is further ramped to 200 °C, the formation of *NS*-TiO$_2$ and rhombic-shaped anatase nanocrystals concurs (Figure 3a and 3b). It should be mentioned that some of the rhombic nanocrystals are not completely grown in the 1-day reaction. The formation of rhombic anatase nanocrystals at 200 °C exhibits a strong dependence on reaction time. The growth of rhombic nanocrystals is evidenced only at reaction times beyond 20 h (Figure S4). The three sets of lattice fringes in the HRTEM image (Figure 3c) give three interplanar distances, corresponding to (101), (−101), and (002) of anatase. The rhombic sheet lies in the (010) plane. The interior angles are in agreement with the angle of (101) and (−101) planes, 43.4° and 136.6°, as calculated from the lattice constants of anatase (tetragonal S.G.: *I*4$_1$/*amd*, Z = 4, a = 0.378 52 nm, c = 0.951 39 nm).[47]

The concurrence of {001} exposed *NS*-TiO$_2$ and {010} exposed *NC*-TiO$_2$ in the same-pot reaction has inspired us to further understand their relationship during reactions. As described above, only pure *NS*-TiO$_2$ forms in the 1-day reaction at 180 °C. Our further experiments reveal that heating this product without opening the reactor at 180 °C for another 2 days or at 200 °C for another day results in the formation of the high-quality rhombic nanocrystals (Figure 4). This observa-

(46) Garnweitner, G.; Tsedev, N.; Dierke, H.; Niederberger, M. *Eur. J. Inorg. Chem.* **2008**, 890–895.
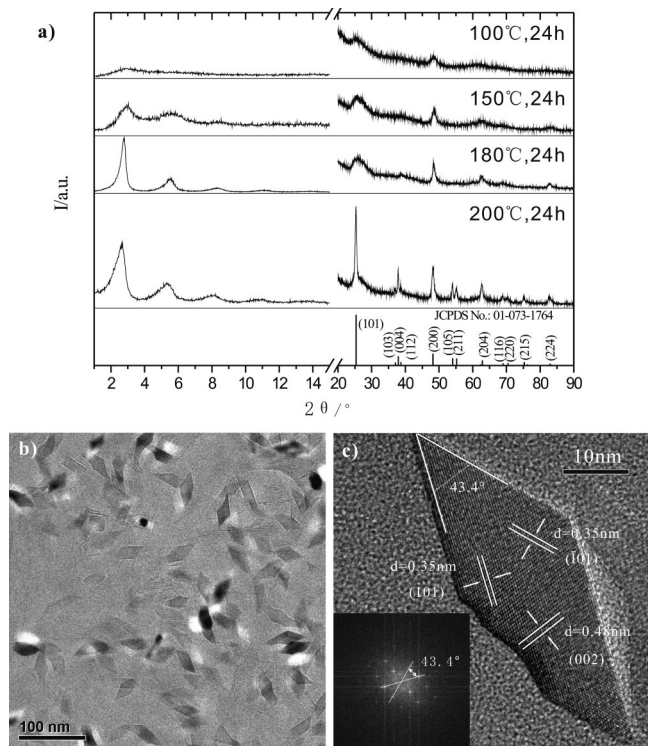(47) Howard, C. J.; Sabine, T. M.; Dickson, F. *Acta Crystallogr., Sect. B* **1991**, *47*, 462–468.

Figure 3. Effect of temperature on synthesis of nanostructured TiO$_2$: (a) XRD patterns of products obtained from the 24-h reactions run at 100, 150, 180, and 200 °C. (b) A low-magnification TEM image of the sample collected from the reaction at 200 °C. (c) A typical HRTEM of TiO$_2$ nanocrystals found in (b). The corresponding Fourier transfer image is shown as inset. Reactions conditions: BA 5 mL, OA 2 mL, TIPO 0.25 mL, no water.

tion might suggest rhombic-shape anatase nanocrystals are essentially converted from the anatase nanosheets which are readily produced at relatively low temperatures under the nonaqueous conditions in our experiments.

Although {010} exposed rhombic-shaped anatase nanocrystals or elongated nanocrystals have been observed in aqueous systems,[8,33,40] they have not yet been obtained in nonaqueous synthesis. In nonaqueous systems, however, the formation of TiO$_2$ nanomaterials normally undergoes mechanisms other than hydrolysis.[21,37,48] In our case, the formation of *NS*-TiO$_2$ would likely result from ether elimination between TIPO and BA. *NS*-TiO$_2$ is then reconstructed and further condensed into rhombic nanocrystals at higher temperatures. Due to its indirect production and lack of purity, the thermal conversion described above is not an ideal process for the large-quantity production of anatase nanocrystals having their {010} facets exposed.

The occurrence of high-quality {010} exposed anatase nanocrystals has demonstrated the possibility to stabilize and prepare them in our nonaqueous systems, which became the driving force for us to seek a better method to achieve their large-scale synthesis in nonaqueous systems. In addition to reaction temperature, we consider water as another important factor to tailor the reactions.[15,34] With the introduction of a trace amount of water, the formation of nanocrystals could undergo a hydrolysis mechanism and therefore pure {010} exposed rhombic anatase nanocrystals can be prepared. Based on this hypothesis, we introduced various amounts of water into the

(48) Garnweitner, G.; Niederberger, M. *J. Mater. Chem.* **2008**, *18*, 1171–1182.
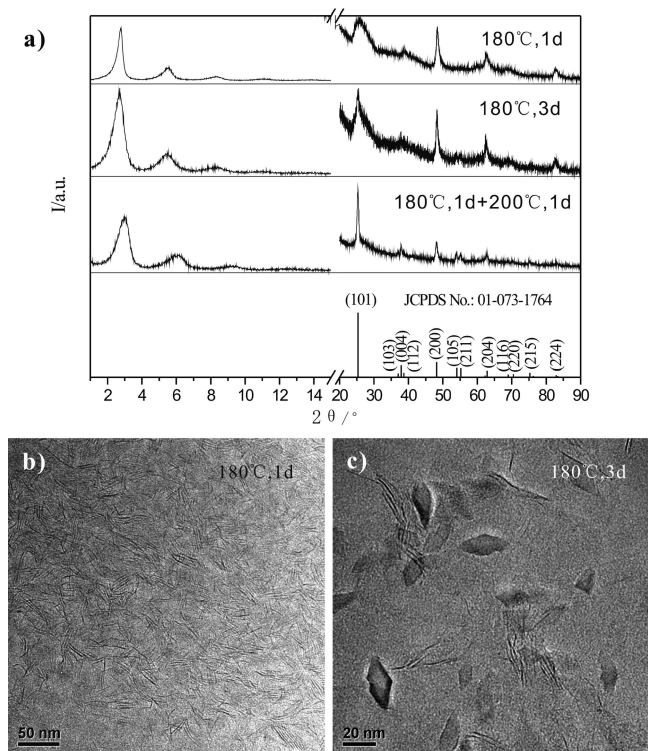
Figure 4. XRD patterns and TEM images of products obtained from reactions run only at 180 °C for 1 day and run at 180 °C for 3 day or 180 °C for 1 day followed by 200 °C for another day. Reaction conditions: BA 5 mL, OA 2 mL, TIPO 0.25 mL, no water.

synthesis of *NS*-TiO$_2$ at 180 °C. As evidenced by XRD, *NS*-TiO$_2$ and *NC*-TiO$_2$ coexist in the reaction containing 0.25 mL of TIPO and 50 μL of water. Pure *NC*-TiO$_2$ is obtained when 60 μL of water are supplied. Further increases of water up to 250 μL do not seem to change the crystal growth of *NC*-TiO$_2$ (Figure 2).

Figure 1d shows a typical TEM image at low magnification of rhombic-shaped *NC*-TiO$_2$ prepared from the reaction with the use of 60 μL of water. Each nanocrystal has a rather homogeneous rhombic sheet texture. An HRTEM image of a selected titania nanocrystal is shown in Figure 1e. Similar to the rhombic anatase nanocrystals grown at 200 °C without the use of water (Figure 3c), three sets of lattice fringes, corresponding to (101), (−101), and (002) of anatase, are clearly revealed. Almost all nanocrystals lie on the TEM grid surface in the {010} plane, which might indicate the thin-plate morphology of the prepared *NC*-TiO$_2$. To confirm the anisotropic growth of *NC*-TiO$_2$ indicated by TEM, we applied XRD to estimate the average crystallite sizes of anatase nanocrystals by using the Sherrer formula. The average crystallite sizes estimated from the measured widths of (101) and (004) reflections are 11.2 and 21.0 nm, respectively. According to TEM analysis, these two sizes correspond to the average side length and long diagonal of the rhombic *NC*-TiO$_2$, respectively. Therefore, crystallite sizes estimated from XRD and TEM are in good agreement. The thickness along the [010] direction is calculated as 5.4 nm using the formula $L(010) = 0.4399L(211)$, where $L(010)$ is the crystallite size in the [010] direction, corresponding to the thickness of the rhombic crystals and $L(211)$ is the crystallite size calculated from the (211) peak.[40] Based on these calculations, we estimate the percentage of {010} facets exposed in *NC*-TiO$_2$ to be 43.4%.
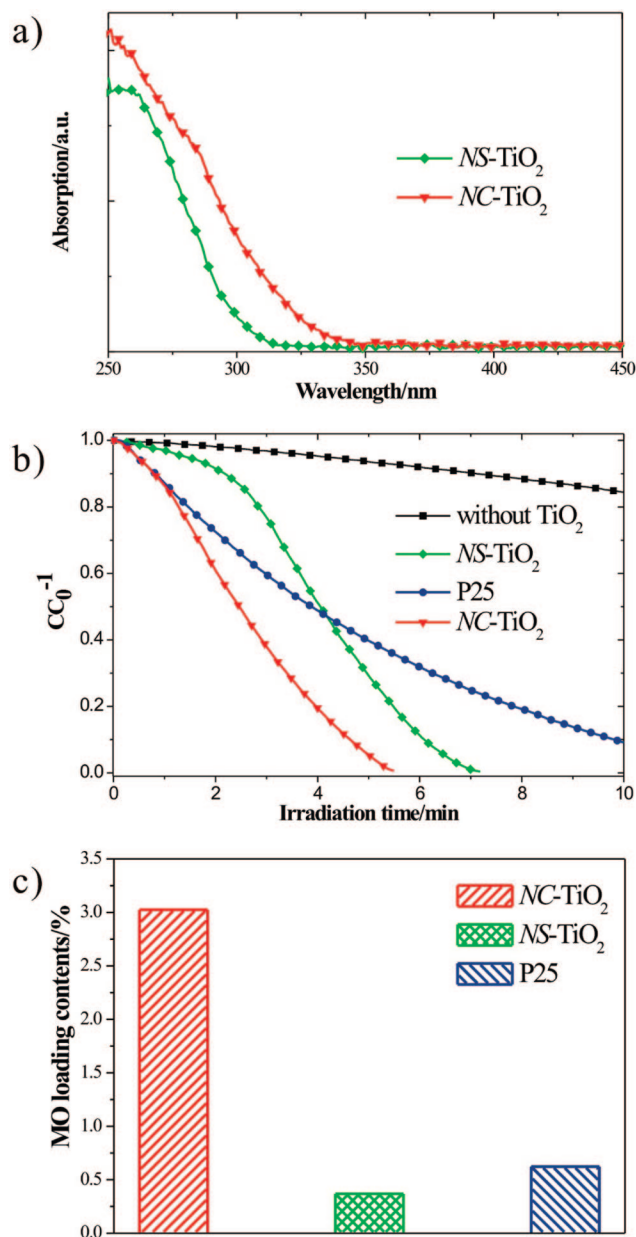
Figure 5. (a) UV−vis spectra of *NS*-TiO$_2$ and *NC*-TiO$_2$ dispersed in chloroform and (b) their photocatalysis performance in degradation of MO in comparison with commercial Degussa P25 TiO$_2$. (c) MO dye adsorption for *NC*-TiO$_2$, *NS*-TiO$_2$, and P25.

In addition to the capability to produce nanocrystals with a morphology that is only observed in aqueous synthesis, another significant feature of the nonaqueous synthetic method we report here is the facile production of uniform nanocrystals in a large quantity since the alkoxide precursor can be used in a concentration as high as 0.68 M. For example, in a reaction containing 5 mL of BA and 2 mL of OA, 2.5 mL of TIPO can be used together with 0.6 mL of H$_2$O to produce 0.728 g of pure *NC*-TiO$_2$. The large-scale production of TiO$_2$ nanostructures with unusual exposed {010} facets has motivated us to investigate their photocatalytic properties.

Based on the UV−vis spectra of *NS*-TiO$_2$ and *NC*-TiO$_2$ samples dispersed in chloroform (Figure 5a), the band gaps of

4.1 and 3.8 eV are calculated for *NS*-TiO$_2$ and *NC*-TiO$_2$, respectively. Their band gaps are both wider than that of bulk anatase (3.2 eV),[49,50] which is due to the quantum confinement effect.[16] Unlike nanocrystals capped by carboxylic acids, as prepared amine-capped *NS*-TiO$_2$ and *NC*-TiO$_2$ are ready to disperse in water after being treated with an ethanol solution of TBAOH. Under the same conditions as those for the photocatalytic degradation of MO, {010} exposed *NC*-TiO$_2$ and {001} exposed *NS*-TiO$_2$ exhibit a conspicuous performance which is better than that of P25 although the induction period required for *NS*-TiO$_2$ is longer than that for P25 (Figure 5b). At the end of photocatalysis measurements, all the TiO$_2$ collected is white and the solutions are colorless, which indicates the full decomposition of MO. Considering that photocatalytic degradation of MO is a complicated process in which absorption on a TiO$_2$ surface is the first step, we carried out 24-h adsorption experiments to compare the adsorption ability of *NS*-TiO$_2$ and *NC*-TiO$_2$ with that of P25. Shown in Figure 5c, the maximum MO adsorption is 3.0%, 0.4%, and 0.6% in weight for treated *NC*-TiO$_2$, *NS*-TiO$_2$, and P25-TiO$_2$, respectively. The excellent degradation ability of *NC*-TiO$_2$ is explained by its superior adsorption properties to *NS*-TiO$_2$ and P25-TiO$_2$ due to the high percentage of {010} exposed surface in *NC*-TiO$_2$.[40] In comparison, TBAOH-treated *NS*-TiO$_2$ has a much lower methyl orange adsorption capacity in the dark. Since methyl orange is negatively charged, the low adsorption ability of *NS*-TiO$_2$ might be attributed to the highly negative charge of the TiO$_2$ sheets as evidenced by Zeta-potential measurements (Figure S5), resulting in the slow initial decomposition rate by *NS*-TiO$_2$. As photocatalysis progresses, the decomposition rate of methyl orange by *NS*-TiO$_2$ increases, which might be caused by the change of surface properties within the TiO$_2$ sheets during reactions.

Conclusions

In conclusion, we have successfully demonstrated a facile nonaqueous synthetic strategy to prepare nanostructured anatase TiO$_2$ with a large percentage of exposed high-energy facets (i.e., {001}, {010}). The strategy is achieved by combining the use of amine capping agents and adscititious water in a nonaqueous alcohol reaction medium. Through such a synthetic strategy, the structural diversity from aqueous systems can be integrated into large-quantity synthesis in nonaqueous systems to create excellent photocatalysts.

Supporting Information Available: XRD patterns of as-prepared *NS*-TiO$_2$ using different amines, the selected area electron diffraction of *NS*-TiO$_2$, TGA curves, Zeta potential measurements. This material is available free of charge via the Internet at http://pubs.acs.org.

(49) Tang, H.; Prasad, K.; Sanjines, R.; Schmid, P. E.; Levy, F. *J. Appl. Phys.* **1994**, *75*, 2042–2047.
(50) Kormann, C.; Bahnemann, D. W.; Hoffmann, M. R. *J. Phys. Chem.* **1988**, *92*, 5196–5201.